REPORT DOCUMENTATION PAGE

1. REPORT DATE *(DD-MM-YYYY)*	2. REPORT TYPE	3. DATES COVERED *(From - To)*
November 2007	Proceedings	June 2007- November 2007

4. TITLE AND SUBTITLE	5a. CONTRACT NUMBER
Role of Superoxide Dismutase in the Photochemical Response of Cultured RPE Cells to Laser Exposure at 413 nm	FA8650-08-D-6930

5b. GRANT NUMBER

5c. PROGRAM ELEMENT NUMBER
062202F

6. AUTHOR(S)	5d. PROJECT NUMBER
	7757
Michael L. Denton, Michael S. Foltz, Kurt J. Schuster, Larry E. Estlack, and Robert J. Thomas	5e. TASK NUMBER
	B2
	5f. WORK UNIT NUMBER
	26

7. PERFORMING ORGANIZATION NAME(S) AND ADDRESS(ES)	8. PERFORMING ORGANIZATION REPORT NUMBER
Air Force Research Laboratory Northrop Grumman Human Effectiveness Directorate 4241 Woodcock Drive Suite B100 Directed Energy Bioeffects Division San Antonio TX 78228 Optical Radiation Branch 2624 Louis Bauer Dr. Brooks City-Base, TX 78235-5128	AFRL 711 HPW/ RHDO

9. SPONSORING / MONITORING AGENCY NAME(S) AND ADDRESS(ES)	10. SPONSOR'S/MONITOR'S ACRONYM(S)
Air Force Research Laboratory Human Effectiveness Directorate Directed Energy Bioeffects Division Optical Radiation Branch 2624 Louis Bauer Dr. Brooks City-Base, TX 78235-5128	711 HPW/ RHDO
	11. SPONSOR'S/MONITOR'S REPORT NUMBER(S)
	AFRL-RH-BR-PC-2007-0024

12. DISTRIBUTION / AVAILABILITY STATEMENT

APPROVED FOR PUBLIC RELEASE; DISTRIBUTION UNLIMITED. PA # 07-392

13. SUPPLEMENTARY NOTES

14. ABSTRACT

Thresholds for photochemical damage were performed in RPE cell lines (artificially pigmented) taken from either human (hTERT-RPE1), wild type (wt) mouse, or transgenic mice deficient (+/-) in either superoxide dismutase 1 (SOD1) or SOD2. The four cell lines were characterized by immunohistochemical and immunoblot analyses to determine relative abundance of the SOD proteins. There was no difference in sensitivity between the human, murine wt and murine SOD1-deficient cells, whereas there was a dramatic (2 fold) increase in threshold irradiance value for the murine SOD2-deficient cells. Possible explanations for the unexpected result are provided.

15. SUBJECT TERMS

photo-oxidation, laser damage threshold, RPE cell, superoxide dismutase

16. SECURITY CLASSIFICATION OF:			17. LIMITATION OF ABSTRACT	18. NUMBER OF PAGES	19a. NAME OF RESPONSIBLE PERSON Samuel Y. O
a. REPORT	**b. ABSTRACT**	**c. THIS PAGE**	SAR	8	19b. TELEPHONE NUMBER *(include area code)*
Unclassified	Unclassified	Unclassified			210-536-3039

Role of Superoxide Dismutase in the Photochemical Response of Cultured RPE Cells to Laser Exposure at 413 nm[‡]

Michael L. Denton[a], Michael S. Foltz[a], Kurt J. Schuster[a], Larry E. Estlack[b], and Robert J. Thomas[c]

[a]Northrop Grumman, Warfighter Concepts and Applications Department, San Antonio, TX, USA, 78228-1330
[b]Conceptual MindWorks, Inc., San Antonio, TX, USA, 78228
[c]Air Force Research Laboratory, AFRL/HEDO, Brooks City-Base, TX, USA, 78235-5214

ABSTRACT

Thresholds for photochemical damage were performed in RPE cell lines (artificially pigmented) taken from either human (hTERT-RPE1), wild type (wt) mouse, or transgenic mice deficient (+/-) in either superoxide dismutase 1 (SOD1) or SOD2. The four cell lines were characterized by immunohistochemical and immunoblot analyses to determine relative abundance of the SOD proteins. There was no difference in sensitivity between the human, murine wt and murine SOD1-deficient cells, whereas there was a dramatic (2 fold) increase in threshold irradiance value for the murine SOD2-deficient cells. Possible explanations for the unexpected result are provided.

Keywords: photo-oxidation, laser damage threshold, RPE cell, superoxide dismutase

INTRODUCTION

Superoxide dismutases (SODs) are a family of enzymes that catalyze the dismutase of two superoxide radicals into one molecule each of hydrogen peroxide and water. The superoxide radical is chemically unstable and has been implicated in contributing to oxygen toxicity via such mechanisms as DNA breakage, hyaluronate depolymerization, and linoleate oxidation.[1] There have been three forms of SOD identified in mammalian cells, each encoded by separate genes.[2] There exists an intracellular and extracellular form of Cu/Zn SOD (SOD1), and the Mn SOD (SOD2) form that localizes in the mitochondrial matrix. The intracellular SOD1 enzyme (the only SOD1 referenced hereafter) is usually described as being distributed throughout the cytoplasm, and although some evidence indicates that it is localized within peroxisomes,[2] this form is excluded from the mitochondria. From genetic studies in yeast, the SOD1 enzyme is involved in regulating oxygen stress from environmental oxidants and hyperoxia; whereas the SOD2 form eliminates respiration-derived superoxide radicals (reference 3 and references therein). From homozygous (-/-) and hemizygous (+/-) knockout studies in the mouse, the lack of SOD1 and SOD2 causes pathology in the central nervous system, cardiomyopathy, and mitochondrial dysfunction (reference 4 and references therein).

[‡] Opinions, interpretations, conclusions, and recommendations are those of the authors and are not necessarily endorsed by the United States Air Force.

Prolonged exposure to non-toxic hyperoxia causes an increase in SOD activity, which correlates with an adaptive ability to tolerate higher oxygen concentrations.[3,5] We have studied photochemical damage to human retinal pigment epithelial (RPE) cells using an artificially pigmented cell culture model.[6-8] When we found in the literature a study of RPE cell cultures from transgenic mice hemizygous for either SOD1 or SOD2,[9] we wanted to use them to assess a possible role of the SOD enzymes in protection from photo-oxidation at 413 nm.

Once we established using Western blot analysis that the SOD-deficient RPE cell lines were indeed deficient in their respective enzyme levels, we compared laser damage thresholds (estimated dose for 50% lethality [ED_{50}]) in each with wild type murine and human RPE cells. Our hypothesis was that SOD-deficiency would lead to an enhanced sensitivity to photo-oxidative damage, and thus decrease the threshold irradiance value compared to cells having a complete complement of SOD enzymes. In light of our paradoxical results, we provide a revised hypothesis which predicts an adaptive response to long-term SOD2-deficiencey.

METHODS
2.1 Cell culture and damage assessment.
The human derived hTERT-RPE1 cell line (BD Biosciences ClonTech Labs, Palo Alto, CA) has been described elswhere.[6-8] Murine RPE cell lines generated from wild-type (wt) B10.A and C57BL6 mice and from mice hemizygous for either SOD2 (SOD2 +/-) or SOD1 (SOD 1+/-) were developed by retroviral transformation with E6/E7 genes of human papilloma virus16 (generous gift from Dr. Ferrington[9]) Except for fetal bovine serum (Atlanta Biologicals, Atlanta, GA), the source for all cell culture media components and buffer solutions was MediaTech, Inc. (Herndon, Virginia). Both human and murine RPE cells were maintained at standard culture conditions (37°C and atmosphere containing 5% CO_2) in DMEM-F12 medium, supplemented with 10% fetal bovine serum, 1 mM glutamine, 100 I.U./ml penicillin, 100 µg/ml streptomycin, 50 µg/ml gentamicin, and 10 mM HEPES buffer (pH 7.4). Cell stock cultures were grown in 75 cm^2 flasks and passaged at confluence (average split ratio of 1:10).

Cells to be used in laser exposure experiments were seeded in 48-well plates at 70,000 cells per well, pigmented the following day with isolated bovine melanosome particles[10] (MPs) such that there were approximately 160 MPs per cell, and exposed on the second day post-seed. Adhering to this schedule (seed wells with cells, add melanosomes, and expose to laser, each on consecutive days) provided monolayers with consistent cell density with >95% viability. No residual MPs were found in growth medium after incubation with the RPE cells.

Cells were exposed to laser irradiation with 100 µL Hank's Balanced Salt Solution (HBSS) in each well. After exposure to laser, this HBSS was replaced with complete growth medium and the cells were placed at standard growth conditions for 1 hr. Finally, cells were assayed for viability using 1.7 µM calcein-AM and 1.4 µM Ethidium homodimer 1 (EthD1) in 0.1 mL HBSS (10 min at 37°C). Exposure sites within wells were identified as positively stained when nuclei were fluorescent with EthD1 (bandpass exciter of 475-545 nm and a barrier filter at 590 nm) and as a region devoid of staining

by calcein-AM (bandpass exciter of 460-490 nm and a bandpass emitter of 490-530 nm). Scoring of damage by three individuals was blind of dosimetry, and a score (yes/no) for damage required a consensus from two. These binary data were input into the Probit software package.[11,12] In addition to probability-dose information (ED_{50}), the Probit output includes uncertainty intervals (fiducial limits at 95% confidence) related to the ED value, and the Probit slope (first derivative at a probability of 0.5 for ED_{50}).

2.2 Western Blot and Immunohistochemical Detection of SOD Enzymes.
For western blot analysis, cells were washed with ice-cold phosphate buffered saline (PBS) and lysed in a cold buffer containing 1% Triton X-100, 20 mM Tris-HCL, pH 7.4, 100 mM NaCl, 0.1 M EDTA, 0.2% SDS, 0.2 mM PMSF and 0.1 mM Leupepsin. The lysate was clarified by centrifugation at 14,000 rpm for 10 min at 4°C. The supernatant was harvested and analyzed for protein content using a bicinchoninic acid (BCA) protein assay kit (PIERCE, Rockford, IL, USA). In preparing samples for electrophoresis, 25 µg of protein per sample were dissolved in sample buffer (5% β-mercaptoethanol, 15% glycerol, 3% SDS, 0.1 M Tris, pH 6.8), boiled for 3 min, and then separated by SDS-PAGE using a mini-gel system (Bio-Rad, CA, USA). The separated proteins were electrophoretically transferred onto polyvinylidene difluoride (PVDF) membranes using a mini blot system (Bio-Rad). The blots were blocked for 2 hr at room temperature with tris-buffered saline (TBS) (10mM Tris, pH 7.5, 100 mM NaCl) containing 5% nonfat dry milk. The blots were washed three times with TBST (10mM Tris, pH 7.5, 100 mM NaCl, 0.05% Tween 20), and then incubated overnight at 4°C with a polyclonal anti-SOD1, anti-SOD2 and anti-β-actin in TBST containing 3% nonfat dry milk. All antibodies were purchased from Santa Cruz Biotech (CA, USA) and diluted to 1:2500 before use. The next day the blots were washed three times with TBST, then incubated 2 hours at room temperature with horseradish peroxidase-conjugated secondary antibodies (1:5000) (Santa Cruz Biotech) in TBST containing 3% nonfat dry milk. After washing three times with TBST, immunoreactive bands were detected by an enhanced chemiluminescence detection kit (PIERCE). Relative protein levels were determined using densitometry (Versa-Doc imaging system, Bio-Rad), normalizing within each lane to the β-actin abundance as internal control.

For immunohistochemical detection of SOD enzymes, RPE cells were detached with trypsin and seeded at 70,000 cells per chamber in BD Falcon chamber slides (35118, BD BioSciences, Bedford, MA) and grown under normal conditions for 2 days post seeding. The cells were washed three times with PBS and fixed in 4% paraformaldehyde (freshly made) for 10 minutes at room temperature, followed by membrane permeabilization by 0.2% Triton X-100 in PBS for 10 minutes at room temperature and washed 3 times with blocking buffer (TBS+5% non-fat dry milk). The cells were washed three times with TBST, and then incubated in a humidity chamber overnight at 4°C with either a polyclonal anti-SOD1 or anti-SOD2 antibodies (1:200 dilution each, Santa Cruz Biotech, CA, USA) in TBST containing 3% nonfat dry milk. The next day, the cells were washed three times with TBST, and incubated for 2 hr at room temperature in a humidity chamber with the appropriate Alexa Fluor 488 secondary antibodies (1:200 dilutions, A11008, Molecular Probes, Eugene, OR) in TBST containing 3% nonfat dry milk. After washing the cells three times with TBST, fluorescence imaging was carried out on an Olympus FluoView300 confocal laser scanning image system (Leeds Instruments, Inc., Irving, TX) using a 20 x water immersion (Olympus XLUMPLFL20XW, N.A. of 0.95) or a 60 x water immersion (Olympus LUMPLFL60XWIR, N.A. of 0.9) objective.

2.3 Lasers, beam delivery, and cell exposures.

A large-frame Krypton laser (Saber-08W-K, Coherent) was used for its 413-nm line. Verification of laser wavelength was performed with a spectrometer (Ocean Optics). Figure 1 provides a schematic representation of the laser delivery to cells in 48-well plates. Attenuation of laser power was achieved by the combination of a half-wave plate ($\lambda/2$) and polarizing beam splitter (Pol). All beams were then co-aligned to a common optical path using apertures and a flip-up mirror (F). The optical path included a telescope (T), a beam shaper (BSh, model GBS-AR14, Newport), a computer-controlled shutter (S), and a single lens (L) imaging system generating a beam diameter of about 0.3 mm (88-mm FL lens) at the cells. The telescope allowed for collimated beam expansion to 4.7 mm prior to entry into the beam shaper, which converted the beam to a flat-top profile. The imaging system was designed to image the beam at the near-field output of the beam shaper (about 8 mm diameter) via 0.05 x magnification. For consistent spot sizes and cleaner flat-top profiles, the beam was passed through an aperture to provide the desired diameter. The effect of the column of HBSS above the cells during exposure was taken into account when determining laser beam diameter (CCD camera and Spiricon software).

Cells were systematically exposed to laser irradiation for 100 s at irradiance ranges useful for determining viability thresholds. The 48-well plates were suspended (without lids) in the beam path using a specialized holder attached to x-y translational stages equipped with computer-controlled motors. Ambient temperature was held constant (35 – 36ºC) throughout the exposures using a novel plexiglass enclosure, which also provided consistent humidity (60 – 70% relative humidity).
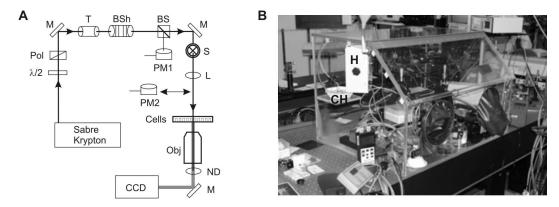

Fig. 1 Laser delivery for *in vitro* damage threshold experiments. Panel A: M, mirror; $\lambda/2$, half-wave plate; Pol, polarizing beam splitter; T, optical telescope; BSh, beam shaper; S, shutter; L, lens; PM, power meter; ND, neutral density filter; CCD, charge-coupled device camera; Obj, microscope objective. Panel B: Photograph of environmentally controlled laser exposure enclosure. H, high capacity air-driven heater; CH, cartridge heater placed in a container of water for generation of humidity.

RESULTS

We used Western blot analysis to determine the relative abundances of the two SOD enzymes in all four RPE cell types. Table 1 provides the quantification results, relative to beta-actin within each lane. The analysis, which artificially sets the protein amounts in the wild type murine cells as 100%, shows that the SOD1-deficient and SOD2-deficient murine cells contained roughly one half of the SOD1 and SOD2 proteins, respectively. Unexpectedly, each SOD-deficient cell type was also slightly deficient in the other SOD protein. It is interesting to note that the human RPE cells had a wide differential in both SOD1 and SOD2 relative to the normal murine RPE cells. The hTERT-RPE1 cells were deficient (about 50%) in SOD1 and over-expressing (about 150%) in SOD2.

Table 1. Quantification of SOD enzymes using Western blot analysis of extracts of cultured human and murine RPE cells (no pigmentation). Quantification by densitometry within each lane was normalized to β-actin, and all SOD protein quantities were then normalized to the amounts found in the wild type (wt) murine cells.

Anti-body	Human RPE cells hTERT-RPE1	Murine RPE cells wt	SOD1(+/-)	SOD2(+/-)
α-SOD1	53 %	100 %	61 %	85 %
α-SOD2	147 %	100 %	91 %	50 %

Immunohistochemistry was used to ensure the antibodies used in the Western blot quantification experiment were consistent with their expected intracellular localization. Figure 2 provides confocal fluorescence micrographs of immunostained human and murine RPE cells.   Notice that in all cases cells had a generalized cytoplasmic fluorescence when stained for SOD1. Conversely, when cells were stained for SOD2, fluorescence was confined to small organelles.   The images were not taken with identical confocal microscope parameters, and thus we could not use this immunohistochemical method to verify intracellular concentration of SOD.
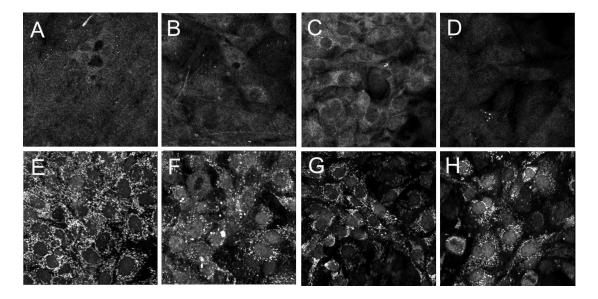
Fig. 2 Immunohistochemical analysis of human and murine RPE cells. Staining for SOD1 (A-D) or SOD2 (E-H). Panels A & E: human RPE cells. Panels B & F: murine wild type RPE cells. Panels C & H: murine SOD1-deficient RPE cells. Panels D & G: murine SOD2-deficient RPE cells.
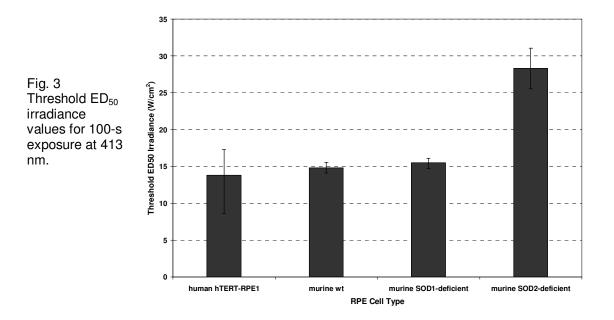
Fig. 3 Threshold ED_{50} irradiance values for 100-s exposure at 413 nm.

Figure 3 shows our ED_{50} threshold study for exposure of the four RPE cell types to photochemical damage. Only the SOD2-deficient cells had a significantly different threshold, which turned out to be nearly double the threshold for the wild-type murine RPE cells. This result indicates a drastic resiliency of these cells, which had about one-half the normal complement of SOD2.

DISCUSSION

To study a possible protective role of SOD enzymes in the photochemical damage pathway(s) using 413-nm laser irradiation, we determined threshold ED_{50} irradiances for the two SOD-deficient murine RPE cell lines, as well as wild-type human and murine RPE cells. Our previous articles[6-8,13-15] have shown that our artificially pigmented hTERT-RPE1 model for laser damage has trends similar trends in action spectra and temporal action profiles from animal studies, and is thus useful in comparative studies such as presented here.

From the comparison of threshold values found in Fig. 3, it is apparent that there was something about the murine SOD2-deficient RPE cells that imparted a strong protective advantage against photo-oxidative damage relative to the other cell lines. A doubling in the damage threshold irradiance is a significant finding. The result seems paradoxical considering the SOD2 enzyme was shown to be reduced to 50% in these cells, relative to the positive control wild-type cells. However, there are other signs that the damage mechanism does not involve the SOD enzymes directly. The results of Table 1 indicate that neither SOD enzyme had a direct role in protecting cells from a 100-s photochemical exposure at 413 nm. Specifically, even though the SOD enzyme concentrations in the human cells were different from the wild-type murine cells by 53% (SOD1) and 147% (SOD2), there was no difference in their sensitivity to photo-oxidative damage. Qualitatively, the results of Table 1 and Fig. 2 are consistent with the specificity described by the manufacturer of the antibodies we used in the Western analyses.

One possible explanation for our result is that within the different RPE cell types there are differences in SOD enzyme specific activity. That is, that a given amount of SOD enzyme in one cell type does not have the same enzyme activity as in another. Or perhaps the α-SOD antibodies used in the Western analysis have widely varying affinities for human and murine SOD proteins. We did not experimentally address these issues here. The immunohistochemical results shown in Fig. 2 serve as a qualitative assessment rather than as a quantification method. However, we did use the same dilutions of the primary and secondary antibodies for all samples.

To explain these results we propose a new hypothesis that states that neither SOD enzymes play an important role in protecting cells against the specific photo-oxidative stresses of laser exposure at 413 nm. Additionally, the continual growth of these murine RPE cells in reduced levels of SOD2 may have caused a compensatory metabolic shift in a different anti-oxidant pathway that imparted protection. There was apparently not a similar adaptive response in cells deficient in SOD1 levels.

We have sent samples of all four RPE cell types described here for transcriptomic analysis with the hope that the baseline transcription profiles will give clues as to why the SOD2-deficient cells were so strongly resistant to laser exposure at 413 nm. From these results, we expect to learn more of the mechanism(s) involved in photochemical damage at this actinic wavelength.

REFERENCES

1. W. Bors, M. Saran, and G. Czapski, in *Biological and Clinical Aspects of Superoxide Dismutase*, W.H. Bannister and J.V. Bannister eds., Elsevier/North-Holland, Amsterdam, pp. 1-31 (1980).
2. G-A. Keller, T.G. Warner, K.S. Steimer, and R.A. Hallewell, "Cu, Zn superoxide dismutase is a peroxisomal enzyme in human fibroblasts and hepatoma cells," *Proc. Natl. Acad. Sci.* **88**, 7381-7385 (1991).
3. A.P.G.M van Loon, B. Pesold-Hurt, and G. Schatz, "A yeast mutant lacking mitochondrial manganese-superoxide dismutase is hypersensitive to oxygen," *Proc. Natl. Acad. Sci.* **83**, 3820-3824 (1986).
4. O.A. Andreassen, R.J. Ferrante, P. Klivenyi, A.M. Klein, L.A. Shinobu, C.J. Epstein, and M. Flint Beal, "Partial deficiency of manganese superoxide dismutase exacerbates a transgenic mouse model of amyotrophic lateral sclerosis," *Annals of Neurology*, **47**, 447-455 (2000).
5. J.A. Fee, "Is superoxide important in oxygen poisoning?," *Trends Biochem. Sci.* **7**, 84-86 (1982).
6. M.L. Denton, M.S. Foltz, L.E. Estlack, D.J. Stolarski, G.D. Noojin, R.J. Thomas, D. Eikum, and B.A. Rockwell, "Damage threshold for exposure to NIR and blue lasers in an in vitro RPE cell system," *Invest Ophthalmol Vis Sci.* **47**, 3065-3073 (2006).
7. Foltz, M.S., N.A. Whitlock, L.E. Estlack, M.A. Figueroa, R.J. Thomas, B.A. Rockwell, and M.L. Denton, "Photochemical damage from chronic 458-nm laser exposures in an artificially pigmented hTERT-RPE1 cell line," Optical Interactions with Tissue and Cells XVII, Proceedings of SPIE **6084**, 15 (2006)**.**
8. M.L. Denton, D.M. Eikum, G.D. Noojin, D.J. Stolarski, R.J. Thomas, R.D. Glickman, B.A. Rockwell, **"**Pigmentation in NIR laser tissue damage," In: Laser and Noncoherent Light Ocular Effects: Epidemiology, Prevention, and Treatment, (B.E. Stuck and M. Belkin eds), SPIE **4953**, 78-84 (2003).
9. D.A. Ferrington, T.N. Tran, K.L. Lew, H. Van Remmen, and D,S. Gregerson, "Different death stimuli evoke apoptosis via multiple pathways in retinal pigment epithelial cells," *Exp. Eye Res.* **83,** 638-650 (2006).
10. A.E. Dontsov, R.D. Glickman, and M. Ostrovsky, "Retinal pigment epithelium pigment granules stimulate the photo-oxidation of unsaturated fatty acids," Fr*ee Radical Biol Med.* **26**, 1436-1446 (1999).
11. C.P. Cain, G.D. Noojin, and L. Manning, "A comparison of various probit methods for analyzing yes/no data on a log scale," USAF School of Aerospace Medicine, Brooks Air Force Base, TX, USAF Technical Report AL/OE-TR-1996-0102 (1996).
12. D.J. Finney, *Probit Analysis*. New York: Cambridge University Press: (1971).
13. M.L. Denton, M.S. Foltz, K.J. Schuster, L.E. Estlack, H.M. Hodnett, G.D. Noojin, R.J. Thomas, "An in vitro model for retinal laser damage," in Optical Interactions with Tissue and Cells XVII, S. L. Jacques and W. P. Roach, Eds., *Proc. SPIE* **6435**, 643515 (2007).
14. M.L. Denton, M.S. Foltz, K.J. Schuster, L.E. Estlack, R.J. Thomas, "Damage threshold for cultured retinal pigment epithelial cells exposed to lasers at 532 nm and 458 nm," *J. Biomed. Opt.* **12**, 034030 (2007).
15. M.L. Denton, M. S. Foltz, K. J. Schuster, Gary Noojin, L. E. Estlack, R. J. Thomas, "An in vitro model that approximates retinal damage threshold trends," *J. Biomed. Opt.,* submitted.